New insights from PIC simulations on the ExB Electron Drift Instability in Hall thrusters

IEPC-2017-216

Presented at the 35th International Electric Propulsion Conference
Georgia Institute of Technology • Atlanta, Georgia • USA
October 8 – 12, 2017

J.P. Boeuf[1]
LAPLACE, Université de Toulouse, CNRS, INPT, UPS, 118 Route de Narbonne, 31062 Toulouse, France

Abstract: A two-dimensional axial-azimuthal Particle-In-Cell model is used to perform a parametric study of the $E \times B$ Electron Drift Instability ($E \times B$ EDI) in the context of Hall thrusters, under simplified conditions. This instability has been observed in recent simulations and analyzed based on the dispersion relation of linear theory. It is characterized by the development of an azimuthal wave with wavelength in the mm range and velocity on the order of the ion acoustic velocity, which enhances electron transport across the magnetic field. In this paper we study the development and convection of the $E \times B$ EDI in the acceleration and near plume regions of a Hall thruster for a given, non self-consistent profile of the ionization source. The results are compared with recent theory and simulations and show that the wavelength and the amplitude of the azimuthal field fluctuations increase with plasma density as the inverse of the Debye length in agreement with the theory. The frequency and wavelength of the instability are consistent with collective light scattering measurements and with theory but the amplitude of the fluctuations is much larger than the measured one. For plasma densities smaller than under nominal conditions of Hall thrusters anomalous cross-field electron transport induced by the $E \times B$ EDI is no longer sufficient and transit time instabilities develop in the axial direction.

Nomenclature

$n, T_e, \lambda_{De}, \Omega_{ce}$	=	plasma density, electron temperature, electron Debye length, electron cyclotron angular frquency
$\omega_{pe}, \omega_{pi}, \omega, \gamma$	=	electron and ion plasma angular frequencies, wave frequency and growth rate of the instability
$\mathrm{v}_{th}, V_d, V_{bi}$	=	electron thermal velocity, azimuthal electron drift velocity, axial ion beam velocity
x, y, z	=	axial, radial, and azimuthal directions
E_x, E_z, B	=	axial and azimuthal components of the electric field, radial magnetic field
$k, k_{\max}, \lambda$	=	wavenumber, wavenumber at maximum growth rate, wavelength
d, w	=	length and width of the thruster channel
$S(x), J_M$	=	ionization rate profile, maximum ion current density $J_M = e\int_0^d S(x), dx$
$\Gamma_{ec}, \Gamma_{ea}, \Gamma_{ic}, \Gamma_{ia}$	=	azimuthally averaged electron and ion fluxes to the cathode and anode sides of the domain
$\Gamma_{ec1}, \Gamma_{ec2}$	=	azimuthally averaged cathode emitted electron fluxes entering the channel and the plume resp.
$J_{ec}, J_{ea}, ...$	=	current densities corresponding to the $\Gamma_{ec}, \Gamma_{ea}, ...$

[1] Senior scientist, CNRS, jpb@laplace.univ-tlse.fr.

I. Introduction

In a Hall thruster, ion acceleration is due to the generation of a large axial electric field in the plasma, resulting from the drop of electron conductivity induced by the presence of a radial magnetic field that efficiently confines the electrons in the exhaust region. The combination of axial electric field E and radial magnetic field B leads to a large ExB electron drift in the azimuthal direction (closed drift). The electron drift velocity, E/B, is on the order of 10^6 m/s i.e. the ratio of electron drift velocity to electron thermal velocity is not small, typically between 0.1 and 1.

It has been known for a long time that the neutral density in the exhaust region of a Hall thruster is too low (by more than a factor of 10) to allow classical electron transport through the magnetic barrier by electron-atom collisions. In the absence of reliable theory, the "anomalous" electron transport in Hall thruster prevents the development of predictive simulation codes and the available fluid models of Hall thrusters use empirical coefficients to describe cross-field electron transport (see [1] and references therein). In this paper, we use a 2D particle simulation to get insight in the physics of anomalous cross-field transport in Hall thrusters.

Particle-In-Cell Monte Carlo Collisions (PIC MCC) simulations performed by Adam et al.[2] have shown that microturbulence can be responsible for anomalous electron transport in the ExB configuration of Hall thrusters. The 2D (axial-azimuthal) PIC MCC simulations showed the development of a small wavelength (in the mm range) azimuthal wave propagating at a velocity close to the ion acoustic velocity (i.e. with frequency in the 1-10 MHz range).

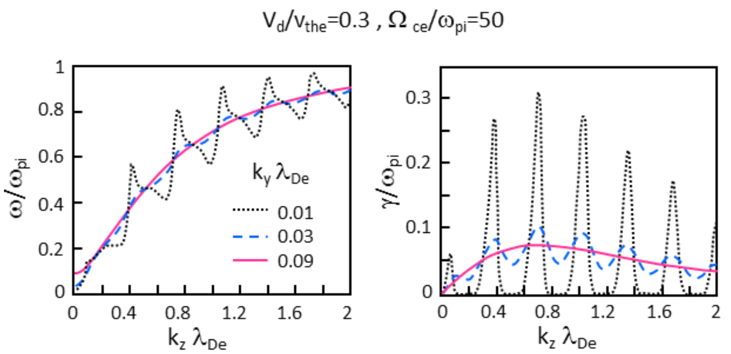

Figure 1: Solutions of the 3D EXB EDI dispersion relation – Adapted from Cavalier at al.[3]. k_z and k_y are the wave vector components in the azimuthal and radial (parallel to B) directions respectively. ω and γ are the real part (angular frequency) and the imaginary part (growth rate) of the instability; ω_{pi} is the ion angular plasma frequency, V_d=E/B the azimuthal drift velocity, v_{the} the electron thermal velocity, Ω_{ce} the electron cyclotron frequency, λ_{De} the electron Debye length. The calculations are made for λ_{De} =8.3x10^{-5} m, ω_{pi} =5.1x10^7 rd/s, (n=2x10^{17} m^{-3}, T_e=25 eV, $V_{i,b}$=16 km/s)

This wave was clearly responsible, in these simulations, for cross-field electron transport in the exhaust region of the thruster (electron-wall interaction and secondary electron emission were not taken into account in the model) and the model was able to reproduce a number of experimental features of Hall thruster operations.

In order to understand the origin of this turbulence, the authors[2, 4] derived the dispersion equation of electrostatic waves in a hot magnetized electron beam drifting across a magnetic field with non-magnetized ions. They showed that in the axial-azimuthal plane and assuming a zero wave vector along the magnetic field, the instability develops in packets of unstable modes ("comb of unstable modes developing for each $k_z V_d = n\Omega_{ce}$", where k_z is the azimuthal wave vector, V_d is the azimuthal electron drift velocity, Ω_{ce} is the electron cyclotron angular frequency, n is an integer). It appeared that the instability present in the PIC simulations was of the same nature as the instability studied in the 1970s in the context of space plasmas and collisionless shocks[5-7].

Cavalier et al.[3] presented a rather complete study of the 3D dispersion relation of instability in the context of Hall thrusters. They concluded that the comb of unstable modes found in the axial-azimuthal plane in Refs. [2, 4] was smoothed out when a non-zero wave vector, k_y , was considered in the direction parallel to the magnetic field. They showed (see Figure 1) that when the parameter k_y increases (even for very low values of $k_y\lambda_{De}$), the dispersion relation tends to an asymptotic curve corresponding to what they called a modified ion acoustic instability. The drift velocity V_d was identified as the mechanism of the instability hence the name "ExB electron drift instability".

Further 1D PIC simulations[8, 9] showed that this instability and the associated anomalous electron conductivity was strongly dependent on the plasma density in the conditions of Hall thrusters (the effective electron mobility increases with increasing plasma density). Lafleur et al.[10] proposed theoretical estimations of the amplitude of the field and plasma density fluctuations assuming that the saturation of the instability was due to ion trapping. The amplitude of the field fluctuations at the maximum growth rate was estimated to vary as $\left|\delta\tilde{E}\right| = \frac{1}{3\sqrt{2}}\frac{T_e}{\lambda_{De}}$ where T_e and λ_{De} are the electron temperature and Debye length, respectively. This gives very large values in the exhaust region, on the order of several 10^4 V/m for standard operating conditions of Hall thrusters (i.e. same order of magnitude as the axial, accelerating electric field.

The 2D axial-azimuthal Particle-In-Cell model of a magnetic barrier described in the present paper is aimed at studying the ExB electron drift instability and associated anomalous electron transport under conditions close to those of a Hall thruster but with simplifying assumptions allowing faster parametric studies. The simplifying assumptions consist in decoupling electron transport from ionization and neutral transport (this strong coupling leads to the low frequency ionization instability in a Hall thruster, not discussed here[1, 11]) by assuming a given ionization source term (axial profile and intensity). The extracted ion current can be modified by changing the intensity of the ionization source term. Changing the position of the ionization source with respect to the magnetic barrier can also help understanding questions associated with the concept of double stage thruster (see Ref. [12]).

In section II we present the principles of the PIC simulations. The results are discussed in section III.

II. Principles of the Axial-azimuthal Particle-In-Cell simulation of the ExB Electron Drift Instability

The aim of this work is to provide a relatively simple parametric study of the ExB EDI. The model is two-dimensional because 3D simulations are not practical for such parametric studies. Since instabilities and turbulence in ExB configurations are most likely to occur in the direction perpendicular to the magnetic field, the simulation domain is in the axial-azimuthal plane (x,z).

The simulation is based on a collisionless Particle-In-Cell (PIC) simulation in the axial-azimuthal plane. Collisions are not described but ionization is taken into account by imposing a given profile of the ionization rate, S(x), in the axial direction x (and uniform in the azimuthal direction). Only a section of the azimuthal direction, of width w is described in the simulation, and we assume periodic boundary conditions in this direction (the total length of the azimuthal direction would be too long – about 30 cm for a 1 kW thruster - for practical simulations). The length of the domain in the axial direction is noted d. In the simulations presented here, w and d are respectively 1 and 2.5 cm.

The simulation domain is shown in Fig. 2.

The electron current is injected from the cathode side of the simulation domain (inside the domain, at a position very close to the right boundary, dashed line on Figure 2) to simulate the presence of an emitting cathode and to ensure current continuity and neutralization of the extracted ion beam. The number of electrons emitted from this location per unit time is equal to the number of electrons minus the number of ions reaching the anode per unit time, as indicated on Figure 2. This way of injecting electrons does not prevent an artificial sheath to form in front of the right boundary (because each electron leaving the domain to the right boundary of the simulation domain is supposed to be lost). In order to fix the plasma potential at the position of electron emission the potential is corrected at each time step by imposing a zero azimuthally averaged potential at the location of electron emission. Doing this, the right boundary is at a negative potential (the drop in potential between the location of electron emission and the right boundary has no useful physical meaning), but the potential drop between the anode and the (azimuthally averaged) potential of the electron emission plane is constant and equal to the applied voltage.

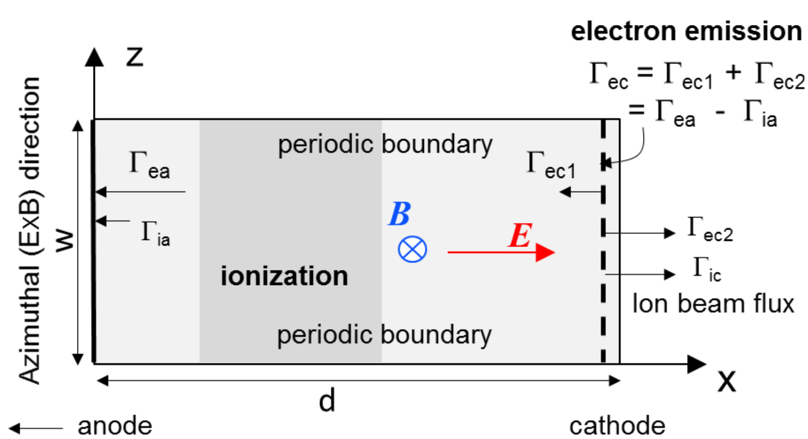

Figure 2: Axial (x) – azimuthal (z) simulation domain. The dimensions w and d are 1 cm and 2.5 cm in the simulations presented here. Electrons are emitted along the dashed line on the cathode side (see text). The darker zone is the ionization region. The azimuthally averged potential on the dashed line (electron emission) is zero and the potential on the left boundary is V. The domain may not contain the "real" anode which is located to the left of the left boundary.

The axial profiles of the magnetic field, B, and of the given ionization rate, S, are shown on Figure 3. The intensity and position of S with respect to the magnetic field can be modified to study the sensitivity of the results to these parameters. The intensity of S controls the maximum ion courant that can be extracted since (continuity equation):

$$\Gamma_{ic} + \Gamma_{ia} = \int_0^d S(x)dx \quad (1)$$

where Γ_{ic} and Γ_{ia} are the absolute values of the azimuthally averaged ion fluxes to the cathode and to the anode boundary (see Figure 2). As said above and indicated on Figure 2, the injected azimuthally averaged electron flux Γ_{ec} must satisfy:

$$\Gamma_{ec} = \Gamma_{ea} - \Gamma_{ia} \quad (2)$$

where Γ_{ea} and Γ_{ia} are the electron and ion fluxes to the anode side (absolute values). The electron flux out of the simulation domain on the cathode side Γ_{ec2} is equal to the ion flux, Γ_{ic}, through the same boundary (this must be a result from the simulation). Finally, the net radially averaged electron flux injected in the channel, Γ_{ec1}, must be such that:

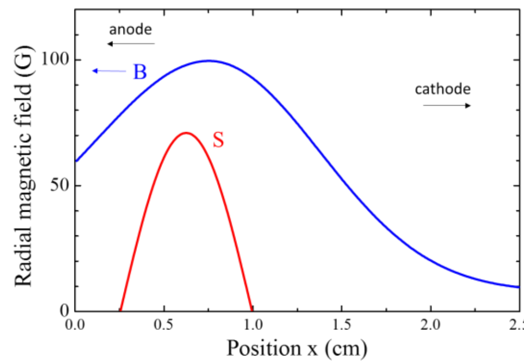

Figure 3: Axial profiles of the radial magnetic field and of the ionization rate in the simulations (the anode region is not described).

$$\Gamma_{ea} = \Gamma_{ec1} + \int_0^d S(x)dx \quad (3)$$

Using eqs. (1) and (3), the net electron flux (or current density) entering the channel from the cathode side, Γ_{ec1} is obtained by measuring Γ_{ea}, Γ_{ia} , and Γ_{ic} in the simulation, i.e.:

$$\Gamma_{ec1} = \Gamma_{ea} - \Gamma_{ia} - \Gamma_{ic} \quad (4)$$

The maximum ion current, J_M, that can be extracted from the channel is related to the ionization rate by:

$$J_M = e(\Gamma_{ic} + \Gamma_{ia}) = e\int_0^d S(x)dx \quad (5)$$

In the simulations shown here, the ionization rate has the spatial profile displayed on Figure 3, and its intensity is varied so that J_M varies between 50 and 400 A/m^2. “Real” Hall thrusters operate (whatever their size) for current densities around 1000 A/m^2 [1, 13]. We chose lower values of the current density to speed up the calculations but we consider that 400 A/m^2 is sufficiently close to real values for the purpose of this simplified approach.

It is known that the contribution of electron-atom collisions to cross-field transport is not sufficient to explain electron conductivity in the region of large magnetic field. Since we are mainly interested in the development of instabilities leading to anomalous electron transport, collisions are not considered in the simulations presented here (and ionization is described by a given rate shown in Figure 3).

The PIC simulation is explicit (i.e. Poisson’s equation is solved at the beginning of each time step and charged particles are moved during one time step assuming that the electric field does not change during that time step). This implies some strong constraints on the grid spacing δx and integration time step δt, which must satisfy[14] $\delta x < \lambda_{De}$ and $\delta t < 0.2/\omega_{pe}$ where λ_{De} and ω_{pe} are respectively the electron Debye length and angular plasma frequency. For the conditions above, with current densities below 400 A/m^2 we found that the Debye length was larger than 50 μm and the plasma frequency was on the order or less than 3x10^{10} s^{-1} so we used a spatial grid of 500x200 and a time step on the order of 0.5x10^{-11} s. The number of charged particles per grid mesh was about 50. The time to reach a steady state regime was, depending on the conditions, as large as several tens of μs and the total computation time for each case presented here was on the order of one to two weeks on a powerful workstation (the PIC code was parallelized and was running on 6 to 12 cores).

III.Parametric study of ExB Electron Drift Instability with axial-azimuthal PIC simulation

The PIC simulation results discussed in this section have been obtained, as said above, with given radial magnetic field and ionization rate profiles (shown in Figure 3), and neglecting collisions between charged particle and neutral atoms (using the ion mass of xenon). The aim is to study the development of instabilities leading to anomalous cross-field electron transport, and to compare the scaling laws obtained with the PIC simulations with those of the ExB EDI.

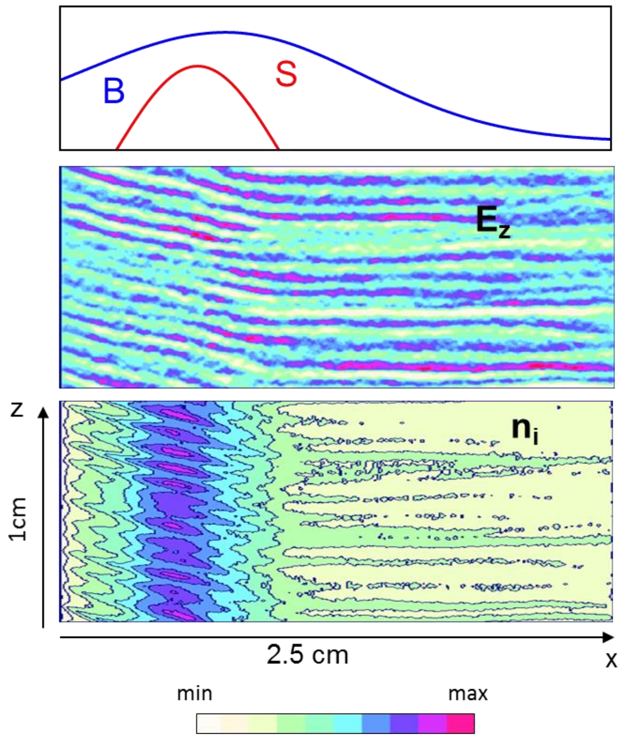

Figure 4: Axial-azimuthal distributions of the azimuthal electric field and of the ion density for J_M =400 A/m^2. The axial distributions of the magnetic field and ionization rate are shown on top of the contour plots. The minimum and maximum values for E_z are -5x10^4 and +5x10^4 respectively, and for n_i are 0 and 5x10^{17} m^{-3}. The applied voltage is 200 V.

The main parameter that is varied in the simulations shown here is the maximum total ion current density J_M that can be extracted from the thruster. This parameter is changed by changing the integral of the ionization rate $J_M = e\int_0^d S(x)dx$ (see eq. (1)) while keeping the same profile (Figure 3).

The simulations are run for a sufficiently long time to reach a steady state (i.e the simulation time is several tens of the ion transit time in the channel). They are started with a uniform quasineutral plasma (initial density of 5x10^{16} m^{-3} in most cases, but the steady results are independent from the initial density). In most situations, we find that the ExB Electron Drift Instability forms in a short time after the acceleration region has formed and the ions have been accelerated. This instability is characterized by the development of an azimuthal wave with large amplitude oscillations of the azimuthal electric field. The frequency of the wave is on the order of the ion acoustic frequency and its wavelength on the order of several Debye length

Figure 4 shows the axial-azimuthal distributions of the azimuthal field and of the ion density at a given time during the wave propagation. As can be seen on this figure, the wavelength is slightly below 1 mm (about 800 μm), i.e. approximately10 times larger than the minimum electron Debye length (about 70 μm in these conditions). The relative amplitude of the ion density oscillations around its average value is as large as 5% (the axial profile of the ion density is aslo shown in Figure 5). The amplitude of the azimuthal field oscillations is also extremely large, on the order of 5x10^4 V/m, i.e. as large as the axial electric field whose axial profile is shown on Figure 5. We also see on Figure 5 the large overlap between the ionization and acceleration regions.

Figure 6 shows the axial-azimuthal distributions of the azimuthal electric field for different values of the maximum extracted ion current density J_M. Note that changing this parameter also changes the value of the plasma density. However, as we will see below, the relation between plasma density and current is not a simple linear relation as one could expect in a quasineutral plasma. The anomalous cross-field electron transport increases with increasing plasma density as was shown in Refs. [8, 9]. We clearly see on Figure 6 that the amplitude and wavelength of the field fluctuations significantly vary with the current (and plasma density). The wavelength and amplitude of the fluctuations increase with decreasing current density (and plasma density). The wavelength roughly varies from 0.8 mm to 1.2, 1.5 and 2. For current densities equal to 400, 200, 100, and 50 A/m^2, respectively, i.e. approximately as the inverse of the square root of the current density. Although, as said above, the relation between plasma density and current density is not a simple linear relation (eg the amplitude of the density fluctuations varies with the current), the azimuthally and time averaged plasma density roughly varies linearly with the current. We can conclude that the wavelength varies as the inverse of the square root of the plasma density, i.e. is roughly proportional to the Debye length. On the other hand, the amplitude of the field fluctuations (see Figure 6) varies as 1.2 x10^4, 2 x10^4, 4x10^4, and 6 x10^4 V/m for current densities equal to 50, 100, 200, and 400 A/m^2 respectively.

The electron temperature (not shown here) does not strongly vary with the current density. Since the simulation is collisionless, the mean electron energy increases as the electric potential from the electron emission plane to the region of ionization where it drops due to the generation of low energy electrons by ionization (ionization rate S).

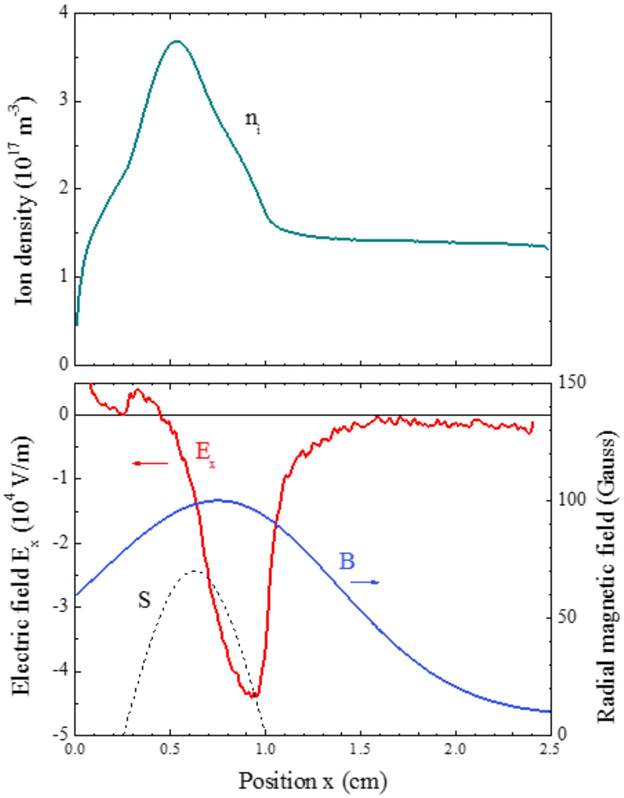

Figure 5: Time averaged axial profiles of the ion density and axial electric field for J_M =400 A/m^2 (same conditions as Figure 4); The radial magnetic field and ionization rate profiles are also shown.

The axial-azimuthal plots of the electric field and plasma densities (Figures 4 and 6) show that the instability is characterized by a dominant wavenumber which depends on the plasma density. One can assume that this wavenumber corresponds the maximum growth rate. From the dispersion curve plotted in Figure 1, the maximum growth rate occurs for $k_z\lambda_{De} \approx 0.7$, which corresponds to a wavelength $\lambda \approx \lambda_{De} 2\pi/0.7 \approx 9\lambda_{De}$. This is consistent with our results which gives a wavelength about 10 times larger than the Debye length (see above).

The theory of this instability[3, 10, 15] shows that it results from electron Bernstein waves which are Doppler-shifted towards low-frequencies by the high drift velocity V_d and merge into an ion acoustic wave. After a few approximations, Lafleur et al. give the following expression for the angular frequency and growth rate of this "modified" ion acoustic wave:

$$\omega \approx k_x \mathrm{V}_{bi} + \frac{kc_s}{\left(1+k^2\lambda_{De}^2\right)^{1/2}} \quad , \; \gamma \approx \sqrt{\frac{\pi m}{8M}} \frac{k_z \mathrm{V}_d}{\left(1+k^2\lambda_{De}^2\right)^{3/2}}$$

(6)

where V_{bi}, c_s, and V_d are respectively the (axial) ion beam velocity, the ion acoustic velocity, and the electron azimuthal drift velocity. The azimuthal wave number $k_{\max}$ giving the maximum growth rate can be obtained from $\partial\gamma/\partial k_z = 0$, which gives $k_{\max} \approx \left(\lambda_{De}\sqrt{2}\right)^{-1}$. This gives a wavelength $\lambda \approx 2\pi\sqrt{2}\lambda_{De}$ (about nine times the electron Debye length) which is consistent with the results from the PIC simulations. The angular frequency and growth rate at the maximum growth rate can then be calculated from the above equations, which gives (for $k_x = 0$):

$$\omega_{\max} \approx \frac{c_s}{\lambda_{De}\sqrt{3}} = \frac{\omega_{pi}}{\sqrt{3}} \text{ , and } \gamma_{\max} \approx \sqrt{\frac{\pi m}{54M}} \frac{\mathrm{V}_d}{\lambda_{De}} = \sqrt{\frac{\pi}{54}} \omega_{pi} \frac{\mathrm{V}_d}{\mathrm{v}_{th}} \quad (7)$$

The wave velocity in the azimuthal direction, $\omega_{\max}/k_{\max} \approx c_s\sqrt{2/3}$ is close to the ion acoustic velocity, while the group velocity (in the axial direction) is $|\partial\omega/\partial \mathbf{k}| \approx V_{bi}$ (this group velocity indicates that the instability is convected at the velocity the ion beam).

The wavelength, wave frequency and velocity from this theory are consistent with the results from the PIC simulations. The orders of magnitude of these parameters, for the conditions of Figure 4 for xenon (plasma density 5x10^{17} m^{-3}, electron temperature 40 eV) are: $\omega_{pi} \approx 8\times10^7$ rd/s, $V_d \approx 4\times10^6$ m/s, $\mathrm{v}_{th} \approx 3\times10^6$ m/s $\omega_{\max} \approx 5\times10^7$ rd/s, $c_s \approx 6\times10^3$ m/s , $\gamma_{\max} \approx 2\times10^7$ s^{-1}. We see that the maximum growth rate of this instability is very large in the conditions of Hall thruster and corresponds to a characteristic growth time lower than 100 ns.

Another important parameter is the amplitude of the fluctuations. The amplitude of the fluctuations cannot be deduced from the dispersion relation since its value depends on the mechanism of saturation of the instability. One possible mechanism of saturation is ion-wave trapping. Previous 1D azimuthal PIC simulations in similar conditions [9](see also Ref.[8]) have shown that ion-wave trapping is the dominant saturation mechanism. Lampe et al.[6, 16] also invokes ion-wave trapping as the saturation mechanism of ion acoustic instability in their theory of beam-cyclotron instability. Ion-wave trapping implies (see, e.g., Lafleur et al.[10] and references therein) that the potential fluctuations, $\delta\tilde{\phi}$, at saturation, are related to the kinetic energy of ions having a velocity equal to the wave velocity by:

$$\delta\tilde{\phi} = \frac{1}{2}\frac{M}{e}\left(\frac{\omega_{max}}{k_{max}}\right)^2 \approx \frac{1}{3}T_e \quad (8)$$

The amplitude of the field fluctuations is therefore:

$$\delta\tilde{E} = k_{max}\delta\tilde{\phi} \approx \frac{1}{3\sqrt{2}}\frac{T_e}{\lambda_{De}} \quad (9)$$

For $T_e = 40$ eV and $\lambda_{De} = 80\ \mu$m (conditions of Figure 4), this gives an amplitude of field fluctuations of about 10^5 V/m which is larger than the simulated values (the expression above can vary by more than a factor of 2, depending on the axial position at which the electron Debye length and electron temperature are estimated in the simulation) but gives the correct order of magnitude. Moreover, the T_e/λ_{De} scaling of the above theory is roughly in agreement with the simulation results of Figure 5.

It is possible to deduce from the PIC simulations the values of the electron current density J_{ec1} entering the channel and which adjusts itself to neutralize the extracted ion beam. Since the beam ion density is fixed by the ion current density and applied voltage, J_{ec1} is directly related to the effective cross-field electron transport and mobility and its value (or the J_{ec1}/J_M ratio) is a measure of the anomalous cross-field transport. Figure 6 shows the variations of J_{ec1}/J_M and J_{ic}/J_M with the imposed maximum ion current density J_M in the conditions of Fig. 5. We see that J_{ec1}/J_M increases quasi-linearly with J_M, which means that the effective electron mobility in the region where the instability is convected increases in the same way with the plasma density. The J_{ic}/J_M ratio slightly decreases with J_M, and is close to 1, meaning that practically all the ions generated in the ionization region are extracted on the cathode side in these conditions (a small fraction reaches the anode).

The value of J_{ec1}/J_M for $J_M = 400$ A/m^2 is quite large. The electron current entering the channel is larger than the extracted ion current. This is not typical of satisfactory operation of a Hall thruster where the electron current entering the channel is expected to be a fraction of the extracted ion current (on the order or less than 30%). This is because the conditions of the simulations are not those of a real Hall thruster (smaller magnetic field, imposed, constant ionization rate, etc…). Nevertheless the simulation results indicate a clear influence of the plasma density on the electron anomalous mobility, and this is correlated with the amplitude of the azimuthal field fluctuations.

Finally we note that for low values of J_M (below 100 A/m^2) the plasma density and current densities are not steady and present low frequency oscillations in the 100 kHz range. These oscillations are associated with the low electron conductivity and correspond to the so-called transit times instabilities (or resistive instabilities, see, e.g., Ref.[17] and references therein). They lead to strong time variations of the energy distribution of the extracted ions, qualitatively similar to those observed in hybrid models of a Hall thruster for low values of the empirical "anomalous transport parameters"[18].

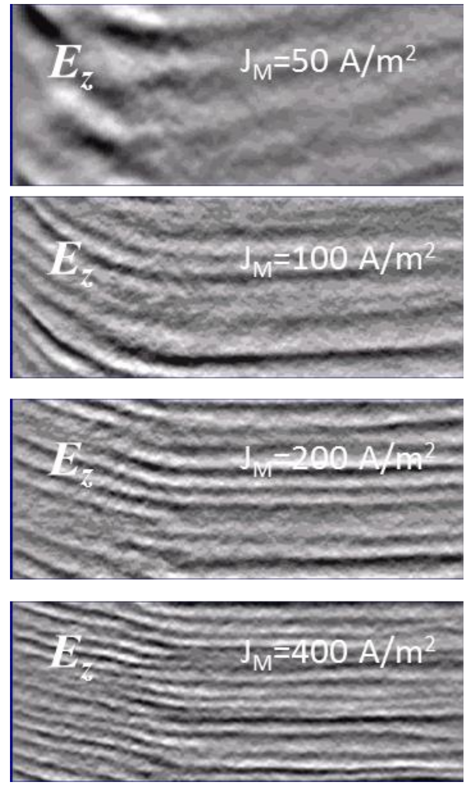

Figure 6: Axial-azimuthal distributions of the azimuthal field for different values of the maximum current J_M. The min-max values of the plotted field are ±1.2x10^4, ±2x10^4, ±4x10^4, and ±6x10^4 V/m for 50, 100, 200, and 400 A/m^2 respectively.

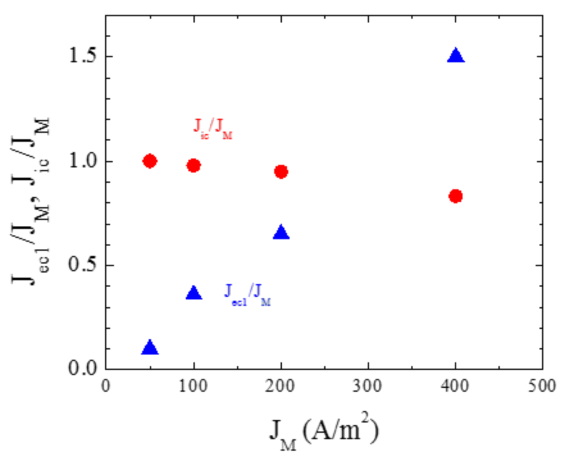

Figure 7: Variations of the ratios of electron current density entering the channel and extracted ion current density to the maximum ion current density (imposed by the given ionization rate) in the conditions of Figure 6.

IV.Conclusion

The results presented in this paper confirm that 2D axial-azimuthal PIC simulations in conditions similar to those of a Hall thruster, predict the formation of an instability in the ExB, azimuthal direction, with wavelength in the mm range. This instability is similar to the electron cyclotron drift instability that has been studied in the conditions collisionless shocks in space plasmas, and is due to the large ExB electron drift in the azimuthal direction (actually to the large difference between electron and ion drift velocities in the azimuthal direction, the ions being practically not magnetized in these conditions). This instability can be called ExB electron drift instability (ExB EDI), as proposed by Cavalier et al.[3].

The ExB EDI instability forms in the acceleration region (where the electron drift velocity is large), and is convected downstream. The instability allows electron transport across the magnetic field in the absence of collisions. The ExB EDI has a very large growth rate in the conditions of Hall thrusters and its presence is ubiquitous in PIC simulations where the azimuthal direction is described.

The dispersion relation and the theory show that the ExB EDI results from electron Bernstein waves Doppler shifted towards low frequencies by the large drift velocity and merging into an ion-acoustic wave. According to this theory, the maximum growth rate of the instability occurs at a wavelength about ten times the electron Debye length ($\lambda = 2\pi\sqrt{2}\lambda_{De}$), which is on the order of 1 mm in the conditions of Hall thrusters. The phase velocity at the maximum growth rate of the wave in the azimuthal direction is close to the ion acoustic velocity, and the angular frequency and growth rate are proportional to the ion plasma frequency. Assuming that the instability saturates due to ion-wave trapping, the amplitude of the fluctuations of the azimuthal electric field vary as $\delta\tilde{E} \approx T_e \Big/ \left(3\sqrt{2}\lambda_{De}\right)$.

The aim of the PIC simulations presented in this paper was to perform a parametric study of the instability observed in the simulations and to compare it with the theory. The problem has been simplified by assuming a given profile of the ionization rate and by neglecting collisions. This allows to eliminate the complexity associated with the ionization instability and subsequent low frequency oscillations, and allow to focus on the ExB EDI.

The results of the PIC simulations are consistent with the theory of the ExB EDI/ion-acoustic instability and the calculated wavelengths and field amplitude oscillations of the instability approximately follow the scaling laws provided by the theory.

These scaling laws predicts that the amplitude of the azimuthal field fluctuations decreases with decreasing plasma density as the inverse of the electron Debye length, i.e. as the square root of the plasma density. For ion beam current densities on the order or 400 A/m^2 (which is smaller but on the same order of magnitude as the current density in standard Hall thrusters) the simulations show that the azimuthal field fluctuations are responsible for anomalous electron transport across the magnetic field. The values of the effective mobility at the entrance of the channel, for a current density on the order of the nominal current density in Hall thrusters are larger but on the order of magnitude of those expected in a Hall thruster (our conditions are not those of optimized Hall thrusters). For lower values of the ion current density (i.e. of the plasma density), below 100 A/m^2 the anomalous electron mobility due to the field fluctuations is no longer sufficient to neutralize in a steady way the extracted ion beam. In these conditions, lower frequency oscillations, which have the characteristics of transit time oscillations.

This paper is another confirmation of the presence of the ubiquitous presence of the ExB EDI in particle simulations under conditions typical to those of Hall thrusters. It also shows that large fluctuations of plasma density and azimuthal field are necessary to provide sufficient cross-field electron transport. Experiments based on laser collective scattering[19] have shown the presence of azimuthal fluctuations of the plasma density in the same wavelength and frequency range as in the PIC simulations and in the ExB EDI theory. However the amplitude of the density fluctuations that have been detected seems to be much smaller than that predicted by the models. Therefore, the question of the saturation of the instability (3D effects ?, effect of wall-collisions ? …) is still open, and more work needs to be done to study the physical phenomena that could limit the growth of the instability. With lack of clear experimental validation, the possible role of the ExB EDI instability in cross-field electron transport in Hall thrusters, although strongly evidenced by the PIC simulations, is still to be demonstrated.

Acknowledgements

The authors would like to acknowledge useful discussions with T. Lafleur and with participants of the ExB2017 workshop https://exb-2017.sciencesconf.org/)

References

1 J.-P. Boeuf, Journal of Applied Physics 121, 011101 (2017).
2 J. C. Adam, A. Héron, and G. Laval, Phys. Plasmas 11, 295 (2004).

[3] J. Cavalier, N. Lemoine, G. Bonhomme, S. Tsikata, C. Honore, and D. Gresillon, Phys. Plasmas 20, 082107 (2013).
[4] A. Ducrocq, J. C. Adam, A. Héron, and G. Laval, Phys. Plasmas 13, 102111 (2006).
[5] S. Gary and J. Sanderson, J. Plasma Physics 4, 739 (1970).
[6] M. Lampe, Phys. Fluids 15, 662 (1972).
[7] E. R. Priest and J. J. Sanderson, Phys. Plasmas 14, 951 (1972).
[8] J. P. Boeuf, Frontiers in Plasma Physics 2, 74 74 (2014).
[9] T. Lafleur, S. D. Baalrud, and P. Chabert, Physics of Plasmas 23, 053502 (2016).
[10] T. Lafleur, S. D. Baalrud, and P. Chabert, Physics of Plasmas 23, 053503 (2016).
[11] J. Boeuf and L. Garrigues, J. Appl. Phys. 84, 3541 (1998).
[12] L. Dubois, F. Gaboriau, L. Liard, D. Harribey, C. Henaux, S. Mazouffre, and C. Boniface, IEPC-2017-215, 35th International Electric Propulsion Conference, Atlanta, Ga (2017).
[13] D. M. Goebel and I. Katz, *Fundamentals of Electric Propulsion: Ion and Hall Thrusters* (Wiley, 2008).
[14] C. K. Birdsall, IEEE Trans. Plasma Sci. 19, 65 (1991).
[15] S. P. Gary and J. J. Sanderson, J. Plasma Phys. 4, 739 (1970).
[16] M. Lampe, W. Manheimer, J. McBride, J. Orens, R. Shanny, and R. Sudan, Phys. Rev. Lett. 26, 1221 (1971).
[17] E. Fernandez, M. K. Scharfe, C. A. Thomas, N. Gascon, and M. A. Cappelli, Phys. Plasmas 15, 012102 (2008).
[18] J. Bareilles, G. J. M. Hagelaar, L. Garrigues, C. Boniface, J. P. Boeuf, and N. Gascon, Physics of Plasmas 11, 3035 (2004).
[19] S. Tsikata, N. Lemoine, V. Pisarev, and D. M. Gresillon, Phys. Plasmas 16 033506 (2009).